Influence of Cu on the catalytic activity of FeBEA zeolites in SCR of NO with NH 3

Pawel Boroń, Lucjan Chmielarz, Stanislaw Dzwigaj

Influence of Cu on the catalytic activity of FeBEA zeolites in SCR of NO with NH_3

Paweł Boroń[1,2,3], Lucjan Chmielarz[1,*], Stanislaw Dzwigaj[2,3,*]

[1]Faculty of Chemistry, Jagiellonian University, Ingardena 3, 30-060 Kraków, Poland

[2]Sorbonne Universités, UPMC Univ Paris 06, UMR 7197, Laboratoire de Réactivité de Surface, F-75005, Paris, France

[3]CNRS, UMR 7197, Laboratoire de Réactivité de Surface, F-75005, Paris, France

*Corresponding authors:

Lucjan Chmielarz, E-mail: chmielar@chemia.uj.edu.pl, tel. +48 12 6632006

Stanislaw Dzwigaj, E-mail: stanislaw.dzwigaj@upmc.fr, tel: +33 1 44272113

Graphical abstract

fx1

Highlights

- Cu and Fe were incorporated into BEA framework as shown by XRD and DR UV-vis.
- In FeSiBEA and CuSiBEA mainly pseudo-tetrahedral Fe(III) and Cu(II) were formed.
- These catalysts showed very high activity in SCR of NO with NH_3.
- 100 % NO conversion and 90 % selectivity toward N_2 at 450-700 K were observed.
- Introduction of Cu in FeBEA had a significant influence on the catalytic activity.

Abstract

Two series of Fe and/or Cu containing BEA zeolites were prepared by different procedures: two-step postsynthesis method (Fe_xSiBEA, Cu_xSiBEA and Fe_xCu_xSiBEA) and conventional wet impregnation ($Fe_xHAlBEA$, $Cu_xHAlBEA$ and $Fe_xCu_xHAlBEA$) (x = 1.0 Fe or Cu wt %).

Modification of BEA zeolite resulted in the incorporation of iron and/or copper into vacant T-atom sites of the zeolite framework as evidenced by XRD and DR UV-vis. Transition metals (Cu or Fe) were incorporated into the framework of BEA zeolite as pseudo-tetrahedral Fe (III) or Cu (II) as proved by XRD, DR UV-vis and TPR investigations. All of obtained zeolite materials were found to be active catalysts of selective catalytic reduction of NO with ammonia. Analysis of NO conversion and catalyst reducibility indicated that the latter played an important role in the $DeNO_x$ process. Co-presence of copper in the zeolite structure decreased the reducibility of iron in Fe_xCu_xSiBEA and Fe_xCu_xHAlBEA, and had significant influence on the low temperature NO conversion.

Keywords: iron, copper, BEA zeolite, ammonia, SCR of NO

1. Introduction

Worldwide environmental regulations regarding NO_x emissions from diesel engines have become significantly more stringent leading to innovative applications of new technologies to resolve this environmental problem. As a potent technology, the selective catalytic reduction (SCR) of NO has been studied intensively [1-4]. Iron and copper based zeolite catalysts are widely employed in selective catalytic reduction of NO with ammonia due to their high temperature durability compared to vanadium based catalysts [5].

Hence, the focus has shifted to the Fe- and Cu-based zeolite catalysts, both of which have demonstrated very high NO reduction efficiencies at high space velocities. The Cu-based catalysts are particularly effective at lower temperatures (< 620 K) [6,7]. Moreover, NO removal efficiencies over the Cu-based catalysts are found to be rather insensitive of the amount of NO_2 in the feed at lower temperatures [7]. On the other hand, the Fe-based catalysts are active at higher temperatures (> 620 K) and give very high NO reduction efficiencies even at very high temperatures (up to 870-970 K) [8,9]. Given the differences in activities of the Cu- and Fe-based catalysts, it seems plausible that a combination of the Fe-zeolite and Cu-zeolite catalysts might achieve high NO conversions over a broader temperature range than the individual catalysts.

A few literature studies considered such combined Fe- and Cu-zeolite systems [10,11,12,13]. Metkar et al. [10,11] studied the combined Fe- and Cu-zeolite monolithic catalysts. The Fe/Cu dual layer catalyst exhibited superior performance for the SCR reaction. Krocher and Elsener [12], who studied double bed catalytic reactors for the SCR reaction, have found that a Fe-zeolite section followed by a Cu-zeolite bed gives higher NO conversion efficiencies. Girard et al. [13] carried out similar studies on combinations of Fe- and Cu-zeolite monolith. They found that the series combinations of (33%) Fe-zeolite followed by (67%) Cu-zeolite gives the highest NO reduction efficiency throughout the studied temperature range. Similar studies on the series of the Fe and Cu-zeolite catalysts with

different individual catalyst lengths were carried out by Theis and McCabe [14]. The approach of the combining of two or more distinct catalysts to achieve the improved performance has been considered in the other reaction systems [e.g. 15]. The other studies [e. g. 16] reported the use of the so-called dual layer monolithic catalysts for SCR of NO with hydrocarbons (e.g. propene) as reducing agents.

Even though the previous studies showed improvements in NO conversion over the Cu and Fe co-exchanged catalysts [10-16], the effect of the preparation method and state of transition metal present in the zeolite structure is not well documented. Usually, transition metal ions are introduced in the extra-framework position of the zeolite structure by ion exchange method. The objective of the earlier studies [10-16] was to determine if the dual-layer Fe/Cu zeolite catalysts can exhibit improved performance for lean NO reduction. Examination of various combinations of the sequential brick and dual layer catalysts was deeply investigated [10,11]. The general aim of the earlier studies [10,11,16] was to systematically vary the lengths of the Fe- and Cu-zeolite monoliths in order to identify superior axial configurations, along the lines of the pioneering studies of Ford Motor Company [17].

Unfortunately, there are only few recent reports that have been focused on the single layer Fe/Cu-catalysts in SCR-NO using NH_3 as a reducing agent. It is worth to note that zeolite containing simultaneously two metal cations was attempted for broadening of the NO conversion temperature window [10,11]. Even though, the previous studies showed improvements in NO conversion over the Cu and Fe co-exchanged catalyst, the effect of variation of Cu/Fe ratio and preparation method is still not well documented.

Thus, in contrast to the previous studies [e.g. 10,11,16], in which the dual layer catalysts were thoroughly investigated, our approach is to obtain single zeolite containing simultaneously two metal cations (Cu and Fe) by two-step postsynthesis and conventional wet impregnation procedures. As it was earlier shown [18,19] for iron and copper, it is possible to

control the incorporation of Fe or Cu into the framework of BEA zeolite using the two-step postsynthesis method. The catalytic activities of FeCuSiBEA and FeCuHAlBEA in SCR-NO with ammonia were compared with the single metal (Fe or Cu) catalysts. The speciation of transition metals in FeCuSiBEA and FeCuHAlBEA zeolites was determined in order to evidence a "structure-properties" relationship in the selective catalytic reduction of NO with NH_3.

2. Experimental

2.1. Materials

Two series of Cu and/or Fe-containing zeolites were prepared by two-step postsynthesis and conventional wet impregnation procedures. Fe_xSiBEA, Cu_xSiBEA and Fe_xCu_xSiBEA zeolites (where x = 1.0 wt % of Fe or Cu, respectively) were prepared by the two-step postsynthesis procedure reported earlier [18,19]. In the first step, 2 g of HAlBEA zeolite, obtained by calcination in air at 823 K for 15 h of tetraethylammonium form of BEA (TEABEA) zeolite (Si/Al = 12.5), provided by RIPP (China) was treated with 13 mol L^{-1} HNO_3 solution under stirring (4 h, 353 K) to remove aluminium from the zeolite structure. In the second step, 2 g of resulting SiBEA (Si/Al = 1000) obtained after filtration were dispersed in aqueous solutions (pH = 2.5) containing 1.8×10^{-3} mol L^{-1} of $Fe(NO_3)_3 \cdot 9\ H_2O$ and/or 1.5×10^{-3} mol L^{-1} of $Cu(NO_3)_2 \cdot 3\ H_2O$ and stirred at room temperature for 24 h. Then, the obtained suspensions were stirred in evaporator under vacuum of a water pump in air at 353 K for 2 h until water was evaporated. The solids with the iron or copper content of 1.0 wt % were labelled as $Fe_{1.0}$SiBEA, $Cu_{1.0}$SiBEA and $Fe_{1.0}Cu_{1.0}$SiBEA, respectively.

Fe_xHAlBEA, Cu_xHAlBEA and Fe_xCu_xHAlBEA zeolites (where x = 1.0 wt % of Fe or Cu, respectively) were prepared by conventional wet impregnation method. Firstly, NH_4AlBEA was calcined in air at 773 K for 3 h to obtain the acidic form of BEA zeolite (HAlBEA). Secondly, 2 g of HAlBEA were dispersed in aqueous solutions (pH = 3.0)

containing 1.8×10^{-3} mol L^{-1} of $Fe(NO_3)_3 \cdot 9\ H_2O$ and/or 1.5×10^{-3} mol L^{-1} of $Cu(NO_3)_2 \cdot 3\ H_2O$ and stirred at room temperature for 24 h. Then, the suspensions were stirred in evaporator under vacuum of a water pump in air at 353 K for 2 h until water was evaporated. The solids with iron or copper content of 1.0 wt % were labelled as $Fe_{1.0}$HAlBEA, $Cu_{1.0}$HAlBEA and $Fe_{1.0}Cu_{1.0}$HAlBEA, respectively.

2.2. Techniques

The structure of the studied samples was determined by powder X-ray diffraction. Diffraction patterns were obtained by a PW 3710 Philips X'pert (Philips X'pert APD) diffractometer using Ni-filtered Cu Kα radiation (λ = 1.54056 Å). The measurements were performed in the range of 2Θ from 5 to 50° with a 0.02° step.

Textural properties of the samples were determined by adsorption of nitrogen at 77 K using a Micromeretics ASAP 2010 apparatus. Prior to nitrogen adsorption all the samples were outgassed, first at room temperature and then at 623 K. The specific surface areas were determined from nitrogen adsorption isotherms in the relative pressure (P/P_0) ranging from 0.05 to 0.16 using BET method, while the micropore volume was determined from the P/P_0 below 0.2.

The DR UV-Vis spectra were recorded using an Evolution 600 (Thermo) spectrophotometer. The measurements were performed in the range of 200-800 nm with a resolution of 2 nm. DR UV-Vis spectroscopy was applied to determine chemical nature of iron and/or copper species in the zeolite structure.

Hydrogen temperature-programmed reduction (TPR) was carried out in a flow of 5% of H_2 in Ar (25 ml/min). The sample was placed in a quartz microreactor and the quantitative consumption of H_2 from 300 to 1120 K (7.5 K/min) was monitored by a TCD detector.

2.3 Catalytic tests

$Fe_{1.0}$SiBEA, $Cu_{1.0}$SiBEA, $Fe_{1.0}Cu_{1.0}$SiBEA, $Fe_{1.0}$HAlBEA, $Cu_{1.0}$HAlBEA and $Fe_{1.0}Cu_{1.0}$HAlBEA were studied as catalysts for SCR of NO with ammonia. Catalytic experiments were performed in a fixed-bed flow microreactor system. The reactant concentrations were continuously measured using a quadrupole mass spectrometer RGA 200 Prevac, with Faraday cup (FC) detector, connected directly to the reactor outlet. Sensitivity of the detector is equal $2 \cdot 10^{-4}$ A/Torr (measured with N_2 28 amu with 1 amu full peak width 10% height, 70 eV electron energy, 12 eV ion energy and 1 mA electron emission current). The minimum detectable partial pressure is about $5 \cdot 10^{-11}$ Torr. Prior to the reaction, each sample (100 mg) of the catalyst was outgassed in a flow of pure helium at 823 K for 30 min. The following composition of the gas mixture was used: [NO] = [NH_3] = 0.25 vol. %, [O_2] = 2.5 vol. % and [He] = 97 vol. %. The reaction was studied in the temperature range between 373 K and 823 K. Total flow rate of the reaction mixture was 40 mL min^{-1}, with a weight hourly space velocity (WHSV) of about 24000 mL h^{-1} g^{-1}.

3. Results and Discussion

3.1. Introduction of iron and copper into BEA zeolite

3.1.1. X-ray diffraction

Figures 1A and 1B present X-ray diffraction patterns of SiBEA, $Fe_{1.0}$SiBEA, $Cu_{1.0}$SiBEA, $Fe_{1.0}Cu_{1.0}$SiBEA (Fig. 1A), HAlBEA, $Fe_{1.0}$HAlBEA, $Cu_{1.0}$HAlBEA and $Fe_{1.0}Cu_{1.0}$HAlBEA (Fig. 1B). The XRD patterns of all the samples are similar and characteristic of BEA zeolite. The crystallinity is preserved after dealumination and the samples do not show any evidence of extra framework crystalline compounds or long-range amorphization of the zeolite structure, as reported earlier [20,21]. Similar XRD diffractograms recorded for all the samples show that introduction of iron and/or copper ions into zeolites do not induce any significant changes in the BEA structure.

The absence of reflections characteristics of extra-framework iron and/or copper oxides in Fe_xSiBEA, Cu_xSiBEA and Fe_xCu_xSiBEA indicates a good dispersion of both Fe and Cu transition metals. It has been reported [22] that a narrow diffraction peak near 22-23° can be used to compare qualitatively lattice contraction/expansion of the BEA structure. An increase of the d_{302} spacing from 3.888 Å (2Θ=22.85°) for SiBEA to 3.939 Å (2Θ=22.55°) and 3.931 Å (2Θ=22.60°) for $Cu_{1.0}$SiBEA upon introduction of 1.0 wt % of Fe and Cu into SiBEA (Fig. 1A) indicates expansion of the matrix as a result of the reaction of iron or copper ions with OH groups of vacant T-atom sites (T = Si or Al) and their incorporation into the framework positions of BEA zeolite, as reported earlier [19,20,21,23]. In spite of this expansion, $Fe_{1.0}$SiBEA and $Cu_{1.0}$SiBEA exhibit similar intensity of diffraction lines as that observed for SiBEA, suggesting that incorporation of Fe and Cu ions into the zeolite framework does not affect their crystallinity. It should be noted that incorporation of both Fe and Cu into SiBEA zeolite results in an increase of the d_{302} spacing from 3.888 Å (2Θ=22.85°) for SiBEA to 3.936 Å (2Θ=22.57°) for $Fe_{1.0}Cu_{1.0}$SiBEA and also proves that iron and copper are incorporated into the BEA zeolite framework.

An introduction of 1.0 wt % of iron or copper into HAlBEA zeolite does not lead to such significant increase in the d_{302} spacing as it was observed upon incorporation of iron ions into SiBEA zeolite (Fig. 1B). In this case, a small increase in the d_{302} spacing from 3.934 Å (2Θ=22.58°) for HAlBEA to 3.946 Å (2Θ=22.51°) for $Fe_{1.0}$HAlBEA and 3.951 Å (2Θ=22.48°) for $Cu_{1.0}$HAlBEA, respectively (Fig. 1B) suggests that only some amounts of iron or copper have been incorporated into the framework of HAlBEA zeolite.

The incorporation of both iron and copper ions into HAlBEA zeolites leads also to a small increase in the interlayer distance in BEA matrix, what results in a shift of a narrow diffraction peak near 22–23° to lower values of 2 theta, from 2Θ=22.58° (d_{302} = 3.934 Å) for HAlBEA to 2Θ=22.53° (d_{302} = 3.943 Å) for $Fe_{1.0}Cu_{1.0}$HAlBEA (Fig. 1B). This effect is

related to the reaction of iron and/or copper ions with OH groups of vacant T-atom sites and their partial incorporation into the framework positions of BEA zeolite.

Moreover, X-ray diffractogram recorded for each sample contains (302) reflection of similar intensity, suggesting that an introduction of Fe and/or Cu into zeolites does not affect their crystallinity.

It should be noted that all materials have similar high BET surface area (620-780 m^2 g^{-1}) and micropore volume (0.19-0.25 cm^3 g^{-1}) characteristic for the BEA structure indicating that textural properties of BEA zeolite are preserved upon dealumination and introduction of iron or copper into BEA structure by two-step postsynthesis procedure as well as by conventional wet impregnation.

3.2. *Nature and environment of iron and copper species in FeBEA, CuBEA and FeCuBEA zeolites*

3.2.1. Diffuse reflectance UV–vis spectroscopy

The nature and environment of iron and copper present in obtained materials have been studied by DR UV-vis spectroscopy (Fig. 2). The white $Fe_{1.0}$SiBEA sample exhibits one band at 248 nm, assigned to oxygen-to-metal charge transfer (CT) transitions involving pseudo-tetrahedral Fe(III), what is in line with earlier results [24-29]. The absence of a broad band near 500 nm, suggests that FeO_x oligomers are not present in $Fe_{1.0}$SiBEA [24-26]. The DR UV-vis spectra of $Cu_{1.0}$SiBEA are composed of a broad and intense band around 845 nm and another band at about 283 nm (Fig. 2A). These bands may be assigned to d–d Cu^{2+} ($3d^9$) and charge transfer (CT) $O^{2-} \rightarrow Cu^{2+}$ transitions, respectively, of isolated Cu(II) in pseudo-tetrahedral coordination, taking into account earlier works on copper in different coordination, environment and crystal field [30-32]. The absence of DR UV-vis bands in the range 300-600 nm, assigned to $O^{2-} \rightarrow Cu^{2+}$ CT transition and/or d–d transition of octa-coordinated Cu(II)

indicates that such copper species are probably not present in $Cu_{1.0}$SiBEA, in line with earlier works [33,34]. For $Fe_{1.0}Cu_{1.0}$SiBEA absorption bands at 275 and 845 nm can be assigned to pseudo-tetrahedral Fe(III) and Cu(II), respectively. It suggests that upon preparation of this sample by two-step postsynthesis method almost all Fe and Cu ions are incorporated in the SiBEA zeolite framework. Fig. 2B shows the DR UV-vis spectra recorded at room temperature for the HAlBEA, $Fe_{1.0}$HAlBEA, $Cu_{1.0}$HAlBEA and $Fe_{1.0}Cu_{1.0}$HAlBEA samples. The $Fe_{1.0}$HAlBEA sample exhibits one band at 280 nm assigned to oxygen-to-metal charge transfer (CT) transitions involving pseudo-tetrahedral Fe(III) [24-26]. Moreover, for this sample a broad band near 400-550 nm is not observed what proves that extra-framework FeO_x oligomers and/or iron oxide are not present. It is in line with earlier studies [35,36]. The DR UV-vis spectrum of $Cu_{1.0}$HAlBEA is composed of a broad band around 845 nm and another less intensive band at 285 nm (Fig. 2B). These bands proves the presence of different kinds of mononuclear Cu(II) [30-32]. The absence of DR UV-vis band in the range 300-600 nm assigned to CT transition of binuclear [32,37] or trinuclear [33] copper-oxygen complexes suggests that such polynuclear complexes are probably not present in $Cu_{1.0}$HAlBEA. For $Fe_{1.0}Cu_{1.0}$HAlBEA, large bands at 280 and 845 nm are observed. These DR UV-vis results show that the catalyst with 1.0 wt % of iron and copper, contains mainly isolated pseudo-tetrahedral Fe(III) and Cu(II) in the framework of BEA zeolite.

3.2.2. Temperature-programmed reduction (TPR)

The reducibility of the Fe(III) and Cu(II) present in $Fe_{1.0}$SiBEA, $Cu_{1.0}$SiBEA, $Fe_{1.0}Cu_{1.0}$SiBEA (Fig. 3A), $Fe_{1.0}$HAlBEA, $Cu_{1.0}$HAlBEA and $Fe_{1.0}Cu_{1.0}$HAlBEA (Fig. 3B) has been investigated by temperature-programmed reduction (TPR) under flowing hydrogen (5 vol % H_2 in Ar). Only one peak at 697 K, probably attributed to the reduction of framework pseudo-tetrahedral iron species from Fe(III) to Fe(II) oxidation state appears for $Fe_{1.0}$SiBEA (Fig. 3A), what is in line with earlier reports [38]. The TPR profile of $Fe_{1.0}$HAlBEA (Fig. 3B) shows two zones of hydrogen consumption: 513-753 K and > 953 K.

As it was reported in previous studies of Fe-ZSM-5 [39], Fe-Y [40] and Fe-BEA [41], the first peak of hydrogen consumption (at 616 K) would correspond to reduction of Fe^{3+} (bare Fe^{3+} cations, and oxo- or hydroxycations) into Fe^{2+}. The high-temperature reduction peak (at 914 K) is ascribed to the reduction of Fe^{2+} to Fe^{0}. H_2-TPR profiles of $Cu_{1.0}$SiBEA and $Cu_{1.0}$HAlBEA are given in Figures 3A and 3B. Two reduction peaks at around 477 and 590 K are detected for $Cu_{1.0}$SiBEA, assigned to reduction of Cu^{2+} to Cu^{+} and Cu^{+} to Co^{0} [42], respectively. While the $Cu_{1.0}$HAlBEA catalyst shows two reduction peaks around 515 and 653 K (Fig. 3B), that can be attributed to one step reduction of Cu^{2+} directly to Cu^{0} and reduction of Cu^{+} to Cu^{0} [42], respectively. $Fe_{1.0}Cu_{1.0}$SiBEA displays a very similar TPR profile as that recorded for $Cu_{1.0}$SiBEA, constituted by a good visible peak centered at ca. 472 K, which proves reduction of Cu^{2+} to Cu^{+}. Moreover, the TPR profile of the catalyst, prepared by two-step postsynthesis method, shows an additional small peak at 624 K corresponding to reduction of Cu^{+} to Cu^{0} and/ or Fe^{3+} into Fe^{2+}. In contrast three main and unresolved peaks at 517, 546 and 590 K, observed for $Fe_{1.0}Cu_{1.0}$HAlBEA prepared by wet impregnation procedure (Fig. 3B), could be attributed to reduction of Cu^{2+} directly to Cu^{0}, framework tetrahedral Fe(III) to Fe(II) and Cu^{+} to Cu^{0}, respectively, in line with earlier work [38,43]. The two additional TPR peaks appearing from 753 to 953 K could be attributed to the reduction of small clusters of Fe_3O_4 to FeO, and then FeO to Fe^{0}, at ca. 777 and 877 K, respectively. The comparison of Figs 3A and 3B reveals that the presence of Cu along with Fe seems to decrease the reducibility of iron as seen from the TPR profiles of the $Fe_{1.0}Cu_{1.0}$SiBEA and $Fe_{1.0}Cu_{1.0}$HAlBEA catalysts.

It should be noted that the physicochemical properties (textural properties, nature of transition metals) determined for all the studied catalysts are collected in Table 1.

3.3. *SCR of NO with NH_3*

Fe and/or Cu containing BEA zeolites have been studied as catalysts for the selective reduction of NO with ammonia. Nitrogen and water vapour are desired products of this process, while N_2O is a side-product. The results of the studies performed for both series of the catalysts are presented in Figs 4 and 5. As it was earlier reported [18], dealuminated SiBEA shows a very low activity and the NO conversion does not exceed 7% in the whole studied temperature range. The NO conversion substantially increases after incorporation of iron in the framework of SiBEA zeolite as pseudo-tetrahedral Fe(III), as shown for $Fe_{1.0}$SiBEA (Fig. 4). It suggests that pseudo-tetrahedral Fe(III), evidenced by DR UV-vis in $Fe_{1.0}$SiBEA (Fig. 2), are responsible for high activity of the catalyst in the SCR of NO process, what is in line with earlier studies [18,44,45]. For $Fe_{1.0}$SiBEA, the NO conversion reaches 100 % with the selectivity to N_2 above 90 % at temperature higher than 673 K. It should be noted that the modification of SiBEA support with copper significantly increases its catalytic activity in the SCR-NO process. The incorporation of Cu into SiBEA leads to its significant catalytic activation (Fig. 4). For the catalyst with 1 wt % of Cu ($Cu_{1.0}$SiBEA), the reaction starts already at 400 K and NO conversion gradually increases with reaction temperature, as shown in Fig. 4. These results confirm that the presence of copper ions in the framework of zeolite is necessary to promote the activity in SCR of NO, in line with earlier report [19]. The incorporation of Cu into SiBEA as isolated pseudo-tetrahedral Cu(II), evidenced by DR UV-vis and TPR investigations (Figs. 2 and 3), leads to obtain a more active catalyst and the main reaction route is the reduction of NO toward N_2. Indeed, for $Cu_{1.0}$SiBEA, a substantial increase of the SCR of NO activity is observed with a maximum NO conversion of 100 % and selectivity to N_2 above 90 % at temperature higher than 473 K. For the $Fe_{1.0}$SiBEA and $Cu_{1.0}$SiBEA catalysts a decrease in effectiveness of NO conversion observed in the high temperature region (above 773 K) is related to the side reaction of direct ammonia oxidation by oxygen, present in the reaction mixture. The $Fe_{1.0}Cu_{1.0}$SiBEA catalyst containing framework pseudo-tetrahedral Fe(III) and Cu(II) (as shown in Fig. 2), presents

much better catalytic activity in SCR of NO than the $Fe_{1.0}$SiBEA and $Cu_{1.0}$SiBEA catalysts (Fig. 4). $Fe_{1.0}Cu_{1.0}$SiBEA shows very high NO conversion in a broad temperature range of 473-623 K. It should be noted that a commercial catalysts for this process, based on V_2O_5–TiO_2 oxide system, operate in a significantly narrower temperature range of 523-673 K [46]. Therefore, these preliminary results obtained in our studies, especially for $Fe_{1.0}Cu_{1.0}$SiBEA are very promising. It should be underline that two-step postsynthesis method applied in this work leads to obtain well-define catalysts, containing isolated framework Fe (III) and Cu (II) sites that play a major role in SCR-NO reaction, as showed earlier [47,48]. Moreover, for $Fe_{1.0}Cu_{1.0}$SiBEA the effect of direct ammonia oxidation is less significant than for $Cu_{1.0}$SiBEA.

Figure 5 shows the NO conversion as a function of the reaction temperature for all catalysts prepared by conventional wet impregnation of HAlBEA ($Fe_{1.0}$HAlBEA, $Cu_{1.0}$HAlBEA and $Fe_{1.0}Cu_{1.0}$HAlBEA). As typical for SCR-NO reaction, a maximum of NO conversion can be found for all these catalysts in a wide temperature window. First of all, it should be noted that the catalytic activity of zeolite without iron (HAlBEA) is rather good, but only in the high temperature region. The NO conversion exceeds ~ 70% with the selectivity to N_2 above 80% at temperature higher than 773 K. The modification of HAlBEA support with iron (1 wt %) in the form of pseudo-tetrahedral Fe (III), significantly increases its catalytic activity in the SCR-NO process. For $Fe_{1.0}$HAlBEA, the NO conversion reaches 100 % with selectivity to N_2 above 90 % at temperature higher than 553 K. The close reaction performance of the $Fe_{1.0}$SiBEA and $Fe_{1.0}$HAlBEA catalysts is in concordance with the similar reducibility of Fe species, deduced from the H_2-TPR experiments (Fig. 3). Results obtained for the sample modified with copper by conventional wet impregnation method are presented in Fig. 5. The $Cu_{1.0}$HAlBEA catalyst achieved 100% NO conversion at temperature 553 K. In agreement with other authors [5,6], $Cu_{1.0}$HAlBEA shows maximum activity at lower temperatures (523-723 K) in comparison with $Fe_{1.0}$HAlBEA (623-783 K). Selectivity to

nitrogen, measured for the $Cu_{1.0}$HAlBEA catalyst, is above 95 %. The activity of $Fe_{1.0}$HAlBEA and $Cu_{1.0}$HAlBEA zeolites is probably related to the presence in both catalyst simultaneously acidic sites and isolated pseudo-tetrahedral Fe(III) or Cu(II) species, as evidenced by TPR and DR UV-vis investigations (Figs. 2, 3) [19,46,49,50,51].

The activity of $Fe_{1.0}Cu_{1.0}$HAlBEA in the SCR-NO process are presented in Fig. 5. For the $Fe_{1.0}Cu_{1.0}$HAlBEA catalyst, NO conversion strongly increases with reaction temperatures and NO is completely converted in the reaction mixture in the range of 473-673 K, with selectivity toward N_2 exceeding 97%. The activity of $Fe_{1.0}Cu_{1.0}$HAlBEA in the reduction of NO with ammonia is influenced by specific iron and copper species, created during modification of HAlBEA zeolite. The framework Cu(II) and Fe(III) present in $Fe_{1.0}Cu_{1.0}$HAlBEA selectively catalyze the formation of nitrogen without undesirable oxidation of ammonia with oxygen at 773 K and at lower temperature, where its activity and selectivity are stable.

The results obtained for all the catalysts allow comparing their activity in the SCR-NO process. The catalytic activities of all the Fe and/or Cu-containing zeolite catalysts are high, however, it should be noted that $Fe_{1.0}Cu_{1.0}$SiBEA and $Fe_{1.0}Cu_{1.0}$HAlBEA are the most active in the low temperature region (T < 473 K), while the catalysts containing only 1.0 Fe wt % or 1.0 Cu wt %, (especially $Fe_{1.0}$SiBEA and $Fe_{1.0}$HAlBEA), show higher activity at elevated temperatures (T > 673 K) (Figs 4, 5). As evidenced by DR UV-vis spectroscopy the Fe-containing zeolite catalysts, obtained by conventional wet impregnation, contain pseudo-tetrahedral Fe(III), while the Cu-containing BEA catalysts contain mainly pseudo-tetrahedral Cu(II) species. Thus, it seems that the presence of these species (isolated framework Fe (III) and Cu (II) in pseudo-tetrahedral coordination) in both kinds of the catalysts ($Fe_{1.0}$SiBEA, $Cu_{1.0}$SiBEA or $Fe_{1.0}$HAlBEA, $Cu_{1.0}$HAlBEA) is responsible for similarity in their high catalytic activity. $Fe_{1.0}Cu_{1.0}$SiBEA and $Fe_{1.0}Cu_{1.0}$HAlBEA zeolites effectively operate in the low and medium temperature range (473-673 K). Additionally, the selectivity towards

nitrogen, measured for these catalysts, is higher than that observed for the samples modified with iron only ($Fe_{1.0}$SiBEA, $Fe_{1.0}$HAlBEA).

It should be underline that the $Fe_{1.0}Cu_{1.0}$SiBEA and $Fe_{1.0}Cu_{1.0}$HAlBEA catalysts show a very high NO conversion in a broad temperature range of 473-623 K. The results of the catalytic tests in SCR-NO provided by Metkar et al., [10,11] and other authors [12,13,14,15,16] are characterized by a very similar performance of the dual-layer and dual-brick catalysts. However, it should be noted that the reaction conditions are different in both cases. The $Fe_{1.0}Cu_{1.0}$SiBEA and $Fe_{1.0}Cu_{1.0}$HAlBEA samples achieve high NO conversions over a broader temperature range and seems to be strong alternative to the dual-layer or sequential brick, catalysts reported earlier [10-16]. Analysis of the catalytic results of $Fe_{1.0}Cu_{1.0}$SiBEA and $Fe_{1.0}Cu_{1.0}$HAlBEA in SCR-NO with NH_3 (Fig. 4,5), have shown that postsynthesis as well as wet impregnation procedure allow to obtain the high-performance single-bed catalysts. It is proved that 1 wt % of transition metals, are optimal to incorporate iron and copper in the zeolite structure as pseudo-tetrahedral Fe(III) or Cu(II) that are responsible for high catalytic efficiency in the SCR-NO process. Moreover, the catalytic performance of studied $Fe_{1.0}Cu_{1.0}$SiBEA and $Fe_{1.0}Cu_{1.0}$HAlBEA, in contradiction to the dual-layer or dual-brick catalysts [10,11], is not decreased by diffusion limitations.

Although the transition metal ions (Fe, Cu) introduces redox properties into the catalysts and modified their acidic properties [52,53], also the reducibility of the metal ions determines degree of NO conversion over the SCR-NO catalysts [54]. The easier is the reduction of the metal species the higher is its oxidation ability. It is worth to notice that the presence of copper along with iron in the $Fe_{1.0}Cu_{1.0}$SiBEA and $Fe_{1.0}Cu_{1.0}$HAlBEA catalysts seems to increase the reducibility of iron species as seen from the TPR profiles (Fig. 3). It is well recognized that in the metal exchanged zeolite catalysts, the reducibility of metal ions determines the extent of the low-temperature NO conversion [55] (Figs 3, 4 and 5).

However, the easily reducible copper species found in the studied catalysts leads to lower NO conversion at high temperatures due to competing undesired NH_3 oxidation reaction (Fig. 4,5). The nitrogen oxide conversion trends in SCR-NO over observed for $Fe_{1.0}Cu_{1.0}$SiBEA and $Fe_{1.0}Cu_{1.0}$HAlBEA are in good agreement with earlier literature reports [56,57]. It should be noted that the presence of Fe and Cu in $Fe_{1.0}Cu_{1.0}$SiBEA or $Fe_{1.0}Cu_{1.0}$HAlBEA, shows different reducibility compared with $Fe_{1.0}$SiBEA, $Fe_{1.0}$HAlBEA or $Cu_{1.0}$SiBEA, $Cu_{1.0}$HAlBEA (Figs 3A, 3B). It seems that temperature window of NO conversion can be controlled by adjusting the reducibility of the studied catalysts. If the low-temperature NO conversion is desired, the presence of copper species seems to be important, whereas for the high-temperature conversion the presence of iron species is desired. As discussed above low temperature NO conversion is mostly determined by the ease of reduction of metal ions, and NH_3 storage has inconsiderable role.

It is suggested in many reports [e.g. 58,59,60] that the oxidation of NO to NO_2 is the rate-limiting step for the SCR-NO reaction. Moreover, according to earlier results [59], the Fe^{3+} ions seem to be responsible for increasing the oxidation rate of NO to NO_2. The earlier published results of NO oxidation by O_2 in the presence of the FeBEA catalysts, obtained by postsynthesis and wet impregnation methods, with framework pseudo-tetrahedral Fe(III) [44] (not shown), proves that the formation of NO_2 is not detected in the studied temperature range (373 to 823 K). Thus, it seems that the reaction step of NO to NO_2 oxidation in the SCR-NO reaction over these catalysts does not play an important role. According to earlier works [45,50,61] and literature data [60,62], it is likely that the SCR-NO reaction mechanism on FeBEA and CuBEA involves the preliminary adsorption of NO that is oxidized by O_2 forming an adsorbed NO_x species (x = 2, 3) bound to a Fe(III) and/or Cu(II) sites. Framework mononuclear Fe(III) and Cu (II) species present in the $Fe_{1.0}Cu_{1.0}$SiBEA and $Fe_{1.0}Cu_{1.0}$HAlBEA catalysts could activate ammonia molecule by abstracting hydrogen atom and then forming an N-oxygenated intermediate species [61]. This active intermediate is

probably responsible for SCR of NO toward N_2 on the studied catalysts, which is in line with earlier report on Co_xSiEA [61]. The recent experimental data obtained by us shows that the nitroethane and acetonitrile adsorbed on FeBEA [45] and CoBEA [61] zeolites are very active and selective in the NO conversion to N_2 and seems to be one of the most probable N-oxygenated intermediate species.

There is still discussion related to possible mechanism of SCR of NO including chemisorption and activation of ammonia molecules as well the nature of active N-complexes. For this reason, further studies are undertaken to determine the mechanism and the role of framework Cu and Fe sites in SCR of NO by temperature programmed studies (e.g. NH_3-TPD-NO, NO-TPD-NH_3, NH_3-TPD, NO-TPD, TPSR and FTIR spectroscopy of adsorbed NO and NH_3). Results of these studies will be presented as a continuation of the current studies.

4. Conclusions

Two series of Fe and/or Cu-containing BEA zeolites prepared by two-step postsynthesis and conventional wet impregnation methods were prepared. Transition metals (Cu or Fe) were incorporated into the framework of BEA zeolite as a framework pseudo-tetrahedral Fe(III) or Cu(II), as proved by XRD, DR UV-vis and TPR investigations.

The catalysts containing simultaneously both iron and copper, $Fe_{1.0}Cu_{1.0}$SiBEA and $Fe_{1.0}Cu_{1.0}$HAlBEA, have been found to efficiently operate in the SCR-NO process in much broader temperature range comparing to the catalysts modified with only one transition metal (Fe or Cu). Moreover, the selectivity to nitrogen obtained over these catalysts was higher than for the process performed in the presence of the other catalysts. It is proved by the analysis of SCR-NO performance that reducibility of obtained catalysts play an important role in the catalytic process.

The higher activity for the $Fe_{1.0}Cu_{1.0}$HAlBEA catalyst compared to $Fe_{1.0}Cu_{1.0}$SiBEA obtained by two-step postsynthesis method, suggested that Fe(III) and Cu (II) species present in the former catalyst, were possibly close to lattice Al, which make them more catalytically active than Fe(III) or Cu (II) species present in siliceous $Fe_{1.0}Cu_{1.0}$SiBEA zeolite.

Simultaneous presence of Cu and Fe in $Fe_{1.0}Cu_{1.0}$SiBEA and $Fe_{1.0}Cu_{1.0}$HAlBEA strongly increases the low temperature NO conversion. Results of SCR-NO with ammonia for $Fe_{1.0}Cu_{1.0}$SiBEA and $Fe_{1.0}Cu_{1.0}$HAlBEA revealed that 1 wt % Cu loading is enough to improve the low-temperature NO conversion. It seems that by varying the amount of Cu and Fe in the catalysts the location of the temperature window of efficient NO conversion could be controlled.

Further studies are underway on the FeCuSiBEA and FeCuHAlBEA catalysts with a higher Cu and Fe content to verify this phenomenon.

Acknowledgements

This research has received funding from the Marian Smoluchowski Kraków Research Consortium - a Leading National Research Centre KNOW supported by the Ministry of Science and Higher Education.

Part of the research was done with equipment purchased in the frame of European Regional Development Fund (Polish Innovation Economy Operational Program - contract no. POIG.02.01.00-12-023/08).

The presented studies were performed in the frame of GDRI programme.

References

[1] L.F. Cordoba, W.M.H. Sachtler, C.M. de Correa, Appl. Catal. B 56 (2005) 269-277.

[2] K. Arve, F. Klingstedt, K. Eranen, J. Warna, L.E. Lindfors, D. Yu. Murzin, Chem. Eng. J. 107 (2005) 215-220.

[3] T. Maunula, J. Ahola, H. Hamada, Appl. Catal. B 26 (2000) 173-192.

[4] D. Tran, C.L. Aardahl, K.G. Rappe, P.W. Park, C.L. Boyer, Appl. Catal. B 48 (2004) 155-164.

[5] R. Delahay, S. Kieger, N. Tanchoux, P. Trens, B. Coq, Appl. Catal. B 52 (2004) 251-257.

[6] T. Komatsu, M. Nunokawa, I.S. Moon, T. Takahara, S. Namba, T. Yashima, J. Catal. 148 (1994) 427-437.

[7] M. Colombo, I. Nova, E. Tronconi, Catal. Today 151 (2010) 223-230.

[8] P.S. Metkar, N. Salazar, R. Muncrief, V. Balakotaiah, M.P. Harold, Appl. Catal. B 104 (2011) 110-126.

[9] R.Q. Long, R.T. Yang, J. Catal. 207 (2002) 224-231.

[10] P.S. Metkar, M.P. Harold, V. Balakotaiah, Appl. Catal. B 111-112 (2012) 67-80.

[11] P. S. Metkar, M. P. Harold, V. Balakotaiah, Chem. Eng. Sci. 87 (2013) 51-66.

[12] O. Krocher, M. Elsener, Ind. Eng. Chem. Res. 47 (2008) 8588-8593.

[13] J. Girard, C. Cavataio, R. Snow, C. Lambert, SAE Paper 2008-01-1185 (2008).

[14] J.R. Theis, R. McCabe, CLEERS Conference, 2008.

[15] A. Obuchi, I. Kaneko, J. Uchisawa, A. Ohi, A. Ogata, G.R. Bamwenda, S. Kushiyama, Appl. Catal. B 19 (1998) 127-135.

[16] C.-S. Kang, Y.-J. You, K.-J. Kim, T.-h. Kim, S.-J. Ahn, K.-H. Chung, N.-C. Park, S. Kimura, H.-G. Ahn, Catal. Today 111 (2006) 229-235.

[17] H.S. Gandhi, H.V. Cavataio, R.H. Hammerle, Y. Cheng, Catalyst system for the reduction of NO_x and NH_3 emissions, United States Patent Application Publication, US 2004/00765465 A1, 2004.

[18] P. Boroń, L. Chmielarz, J. Gurgul, K. Łątka, T. Shishido, J.-M. Krafft, S. Dzwigaj, Appl. Catal. B 138-139 (2013) 434-445.

[19] S. Dzwigaj, J. Janas, J. Gurgul, R. P. Socha, T. Shishido, M. Che, Appl. Catal. B 85 (2009) 131-138.

[20] S. Dzwigaj, M.J. Peltre, P. Massiani, A. Davidson, M. Che, T. Sen, S. Sivasanker, Chem. Commun. 1 (1998) 87-88.

[21] S. Dzwigaj, P. Massiani, A. Davidson, M. Che, J. Mol. Catal. A: Chem. 155 (2000) 169-182.

[22] M.A. Camblor, A. Corma, J. Pérez-Pariente, Zeolites 13 (1993) 82-87.

[23] J. Janas, J. Gurgul, R.P. Socha, J. Kowalska, K. Nowinska, T. Shishido, M. Che, S. Dzwigaj, J. Phys. Chem. C 113 (2009) 13273- 13281.

[24] S. Bordiga, R. Buzzoni, F. Geobaldo, C. Lamberti, E. Giamello, A. Zecchina, G. Leofanti, G. Petrini, G. Tozzola, G. Vlaic, J. Catal. 158 (1996) 486-501.

[25] H. Tippins, Phys. Rev. B 72 (1970) 279-297.

[26] P. Wu, T. Komatsu, T. Yashima, Microporous Mesoporous Mater. 20 (1998) 139-147.

[27] M. Schwidder, S. Heikens, A. De Toni, S. Geisler, M. Berndt, A. Bruckner, W. Grunert, J. Catal. 259 (2008) 96-103.

[28] P. Balle, B. Geiger, S. Kureti, Appl. Catal. B 85 (2009) 109-119.

[29] M.S. Kumar, M. Schwidder, W. Grunert, U. Bentrup, A. Bruckner, J. Catal. 239 (2006) 173-186.

[30] G. Moretti, C. Dossi, A. Fusi, S. Recchia, R. Psaro, Appl. Catal. B 20 (1999) 67-73.

[31] H. Praliaud, S. Mikhailenko, Z. Chajar, M. Primet, Appl. Catal. B 16 (1998) 359-374.

[32] M.H. Groothaert, P.J. Smeets, B.F. Sels, P.A. Jacobs, R.A. Schoonheydt, J. Am. Chem. Soc.127 (2005) 1394-1395.

[33] K.I. Shimizu, R. Maruyama, T. Hatamachi, T. Kodama, J. Phys. Chem. C 111 (2007) 6440-6446.

[34] E.I. Solomon, P. Chen, M. Metz, S. Lee, A.E. Palmer, Angew. Chem. Int. Ed. (2001) 4570-4590.

[35] L. Capek, V. Kreibich, J. Dedecek, T. Grygar, B. Wichterlova, Z. Sobalik, J.A. Martens, R. Brosius, V. Tokarova, Microporous Mesoporous Mater. 80 (2005) 279-289.

[36] M. S. Kumar, M. Schwidder, W. Grunert, U. Bentrup, A. Bruckner, J. Catal. 239 (2006) 173-186.

[37] M.H. Groothaert, J.A. Van Bokhoven, A.A. Battiston, B.M. Weckhuysen, R.A. Schoonheydt, , J. Am. Chem. Soc.125 (2003) 7629- 7640.

[38] B. Coq, M. Mauvezin, G. Delahay, S. Kieger J. Catal. 195 (2000) 298-303.

[39] H.Y. Chen, W.M.H. Sachtler, Catal. Today 42 (1998) 73-83.

[40] J. Novakova, L. Kubelkova, B. Wichterlova, T. Juska, Z. Dolejsek, Zeolites 2 (1982) 17-22.

[41] M. Mauvezin, G. Delahay, B. Coq, S. Kieger, J.C. Jumas, J. Olivier Fourcade, J. Phys. Chem. B 105 (2001) 928-935.

[42] R. Bulanek, B. Wichterlova, Z. Sobalik, J. Tichy, Appl. Catal. B 31(2001) 13-25.

[43] T.V. Voskoboinikov, H.Y. Chen, W.M.H. Schalter, Applied Catalysis B 19 (1998) 279-287.

[44] P. Boroń, L. Chmielarz, J. Gurgul, K. Łątka, B. Gil, J-M. Krafft, S. Dzwigaj, Catal. Today 235 (2014) 210-225.

[45] P. Boroń, L. Chmielarz, J. Gurgul, K. Łątka, B. Gil, B. Marszałek, S Dzwigaj, Microporous Mesoporous Mater. 203 (2015) 73-85.

[46] G. Busca, L. Lietti, G. Ramis, F. Berti, Appl. Catal. B 18 (1998) 1-36.

[47] R. Long, R. Yang, Journal of the American Chemical Society 121 (1999) 5595-5596.

[48] R. Long, R. Yang, Catal. Lett. 74 (2001) 201-205.

[49] H. Bosch, F. Janssen, Catal. Today 2 (1988) 369-379.

[50] J. Janas, J. Gurgul, R. Socha, S. Dzwigaj, Appl. Catal. B 91 (2009) 217-224.

[51] K. H. Rhee, F. R. Brown, D. H. Finseth, J. M. Stencel, Zeolites 3 (1983) 334-338.

[52] S. Kieger, G. Delahay, B. Coq, B. Neveu, J. Catal. 183 (1999) 267-280.

[53] G. Centi, G. Gollinetti, G. Busca, J. Phys. Chem.. 94 (1990) 6813-6819.

[54] M. Koebel, M. Elsner, Chem. Eng. Sci. 53:4 (1998) 657-669.

[55] K. Arakawa, S. Matsuda, H. Kinoshita, Applied Surface Science 121-122 (1997) 382.

[56] A. Grossale, I. Nova, E. Tronconi, Journal of Catalysis 265 (2009) 141-147.

[57] A.Z. Ma, W. Grunert, Chemical Communications (1999) 71-72.

[58] J. Eng, C. H. Bartholomew, J. Catal. 171 (1997) 27-44.

[59] R. Q. Long, R. T. Yang, J. Catal. 188 (1999) 332-339.

[60] N.W. Cant, I.O.Y. Liu, Catal. Today 63 (2000) 133-146.

[61] J. Janas, T. Machej, J. Gurgul, R.P. Socha, M. Che, S. Dzwigaj, Appl. Catal. B 75 (2007) 239-248.

[62] R. Burch, J.P. Breen, F.C. Meunier, Appl. Catal. B 39 (2002) 283-303.

Figure captions

Figure 1. XRD patterns recorded at room temperature of SiBEA, $Fe_{1.0}$SiBEA, $Cu_{1.0}$SiBEA, $Fe_{1.0}Cu_{1.0}$SiBEA (A), and HAlBEA, $Fe_{1.0}$HAlBEA, $Cu_{1.0}$HAlBEA, $Fe_{1.0}Cu_{1.0}$HAlBEA (B).

Figure 2. DR UV-vis spectra recorded at ambient atmosphere of SiBEA, $Fe_{1.0}$SiBEA, $Cu_{1.0}$SiBEA, $Fe_{1.0}Cu_{1.0}$SiBEA (A), and HAlBEA, $Fe_{1.0}$HAlBEA, $Cu_{1.0}$HAlBEA, $Fe_{1.0}Cu_{1.0}$HAlBEA (B).

Figure 3. H_2-TPR profiles of SiBEA, $Fe_{1.0}$SiBEA, $Cu_{1.0}$SiBEA, $Fe_{1.0}Cu_{1.0}$SiBEA (A), and HAlBEA, $Fe_{1.0}$HAlBEA, $Cu_{1.0}$HAlBEA, $Fe_{1.0}Cu_{1.0}$HAlBEA (B).

Figure 4. NO conversion and N_2 selectivity in SCR of NO with NH_3 on SiBEA, $Fe_{1.0}$SiBEA, $Cu_{1.0}$SiBEA, $Fe_{1.0}Cu_{1.0}$SiBEA.

Figure 5. NO conversion and N_2 selectivity in SCR of NO with NH_3 on HAlBEA, $Fe_{1.0}$HAlBEA, $Cu_{1.0}$HAlBEA, $Fe_{1.0}Cu_{1.0}$HAlBEA.

Table 1. The physicochemical properties of studied catalysts.

SAMPLE	Specific surface area S_{BET} (m^2/g)	t-plote Micropore Area (m^2/g)	t-plote Micropore Volume (cm^3/g)	wt % of Fe	wt % of Cu	Nature of Fe/Cu species
SiBEA	789.7	625.7	0.24	0.019	0.002	-
$Fe_{1.0}$SiBEA	714.2	537.5	0.21	1.000	-	pseudo-Td Fe^{3+}
$Cu_{1.0}$SiBEA	764.0	588.2	0.23	-	1.000	pseudo-Td Cu^{2+}
$Fe_{1.0}Cu_{1.0}$SiBEA	660.6	508.7	0.20	1.000	1.000	framework pseudo-Td Fe^{3+} and Cu^{2+}
HAlBEA	727.8	565.0	0.22	0.027	0.002	-
$Fe_{1.0}$HAlBEA	647.1	522.3	0.21	1.000	-	pseudo-Td Fe^{3+}
$Cu_{1.0}$HAlBEA	635.0	490.8	0.19	-	1.000	mononuclear Cu^{2+}
$Fe_{1.0}Cu_{1.0}$HAlBEA	616.9	497.2	0.20	1.000	1.000	pseudo-Td Fe^{3+} and Cu^{2+}

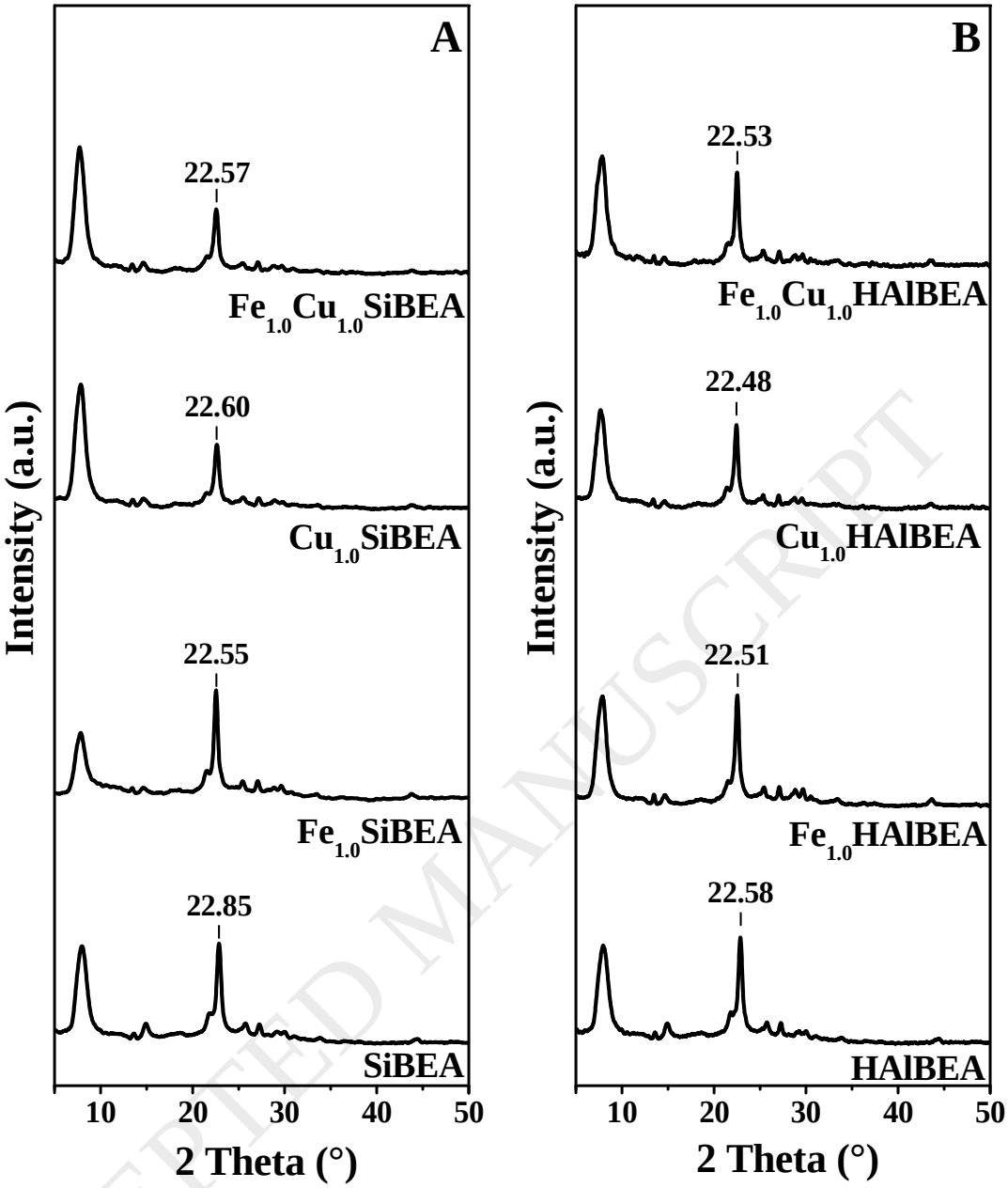

Fig. 1

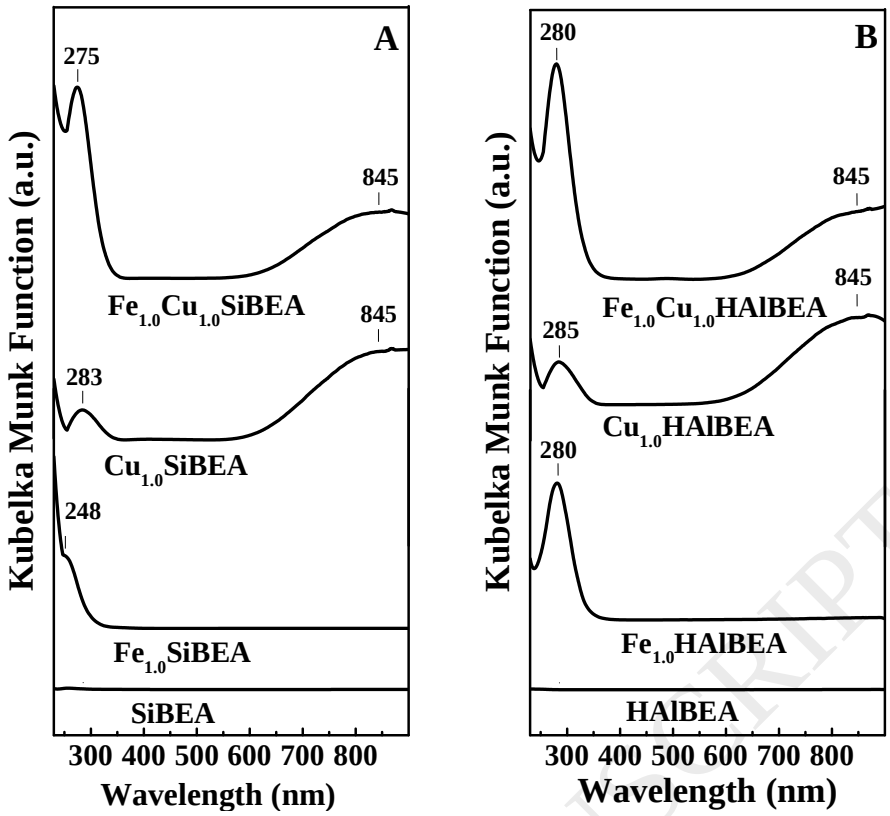

Fig. 2

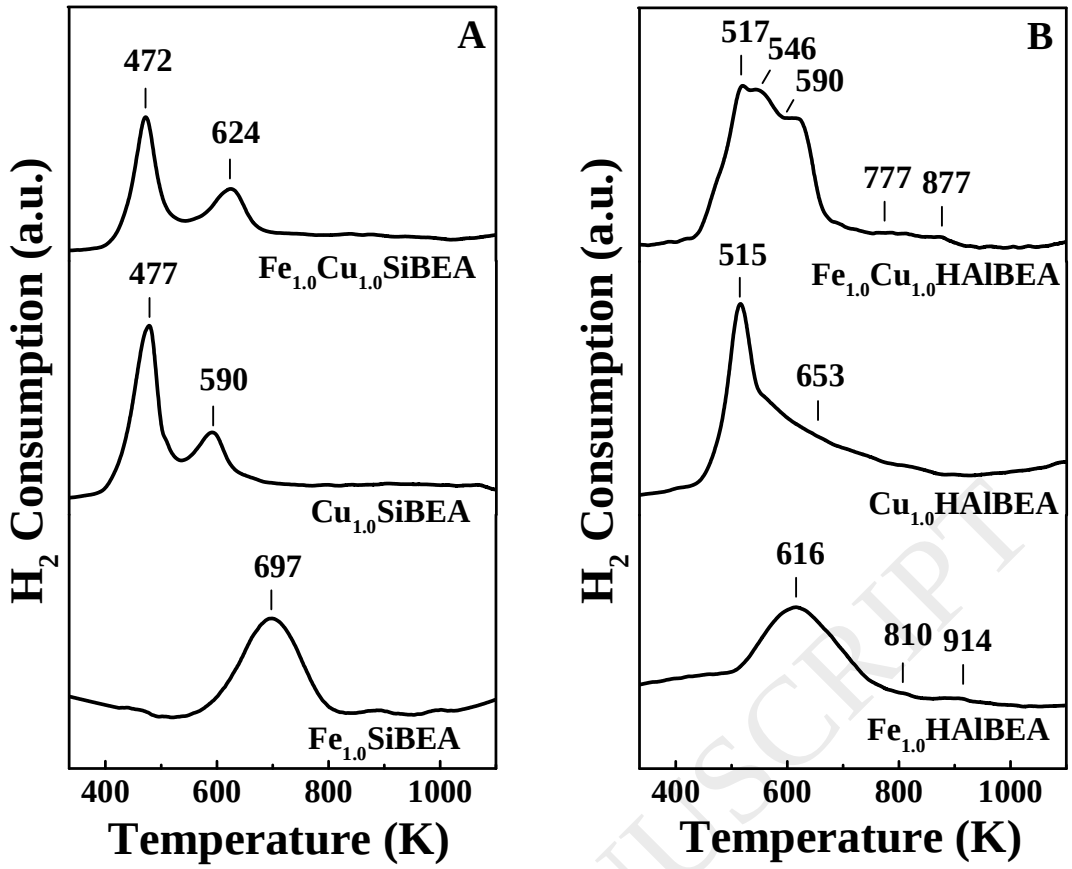

Fig. 3

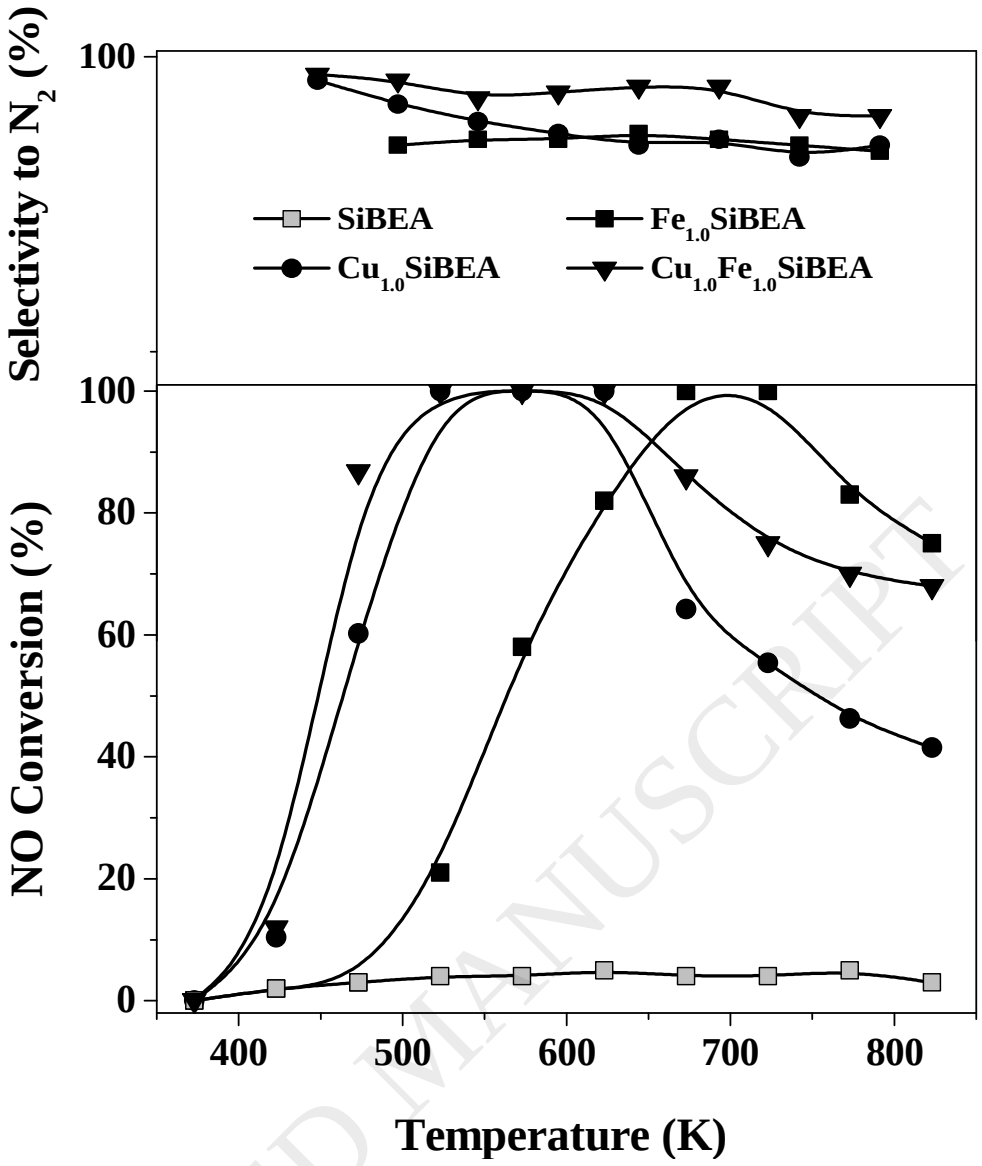

Fig. 4

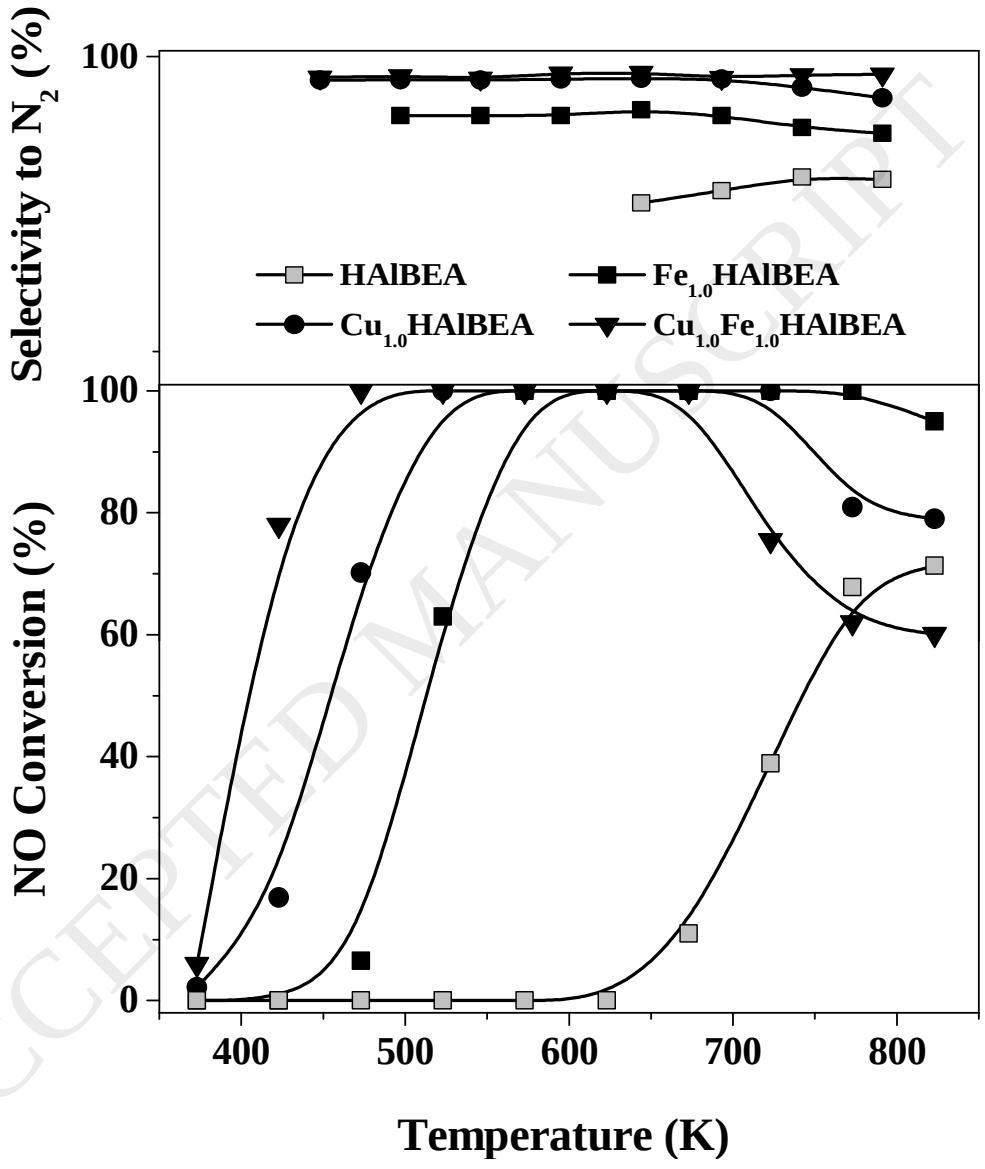

Fig. 5